

# **Analysis of Cloud Spectral Radiance/Irradiance at the Surface and Top-of-the-Atmosphere from Modeling and Observations**

*Z. Li and A. Trishchenko  
Canada Centre for Remote Sensing  
Ottawa, Ontario, Canada*

*M. Cribb  
Intermap Technologies Ltd.  
Ottawa, Ontario, Canada*

## **Introduction**

In view of some reported discrepancies concerning cloud parameter retrievals and cloud absorption (Stephens and Tsay 1990; Li et al. 1999; Rossow and Schiffer 1999) it is useful to compare cloud spectral signatures derived from modeling and observations. This may uncover problems and critical factors important for better understanding cloud-radiation interaction and the earth's solar radiation budget. The review by Stephens and Tsay (1990) postulated several possible causes for the purported excess cloud absorption including uncertainties associated with synergetic measurements of solar fluxes below and above a cloud layer, model input parameters and effects of inhomogeneity on the determination of net fluxes. Li et al. (1999) underscored the importance of data quality issues, in particular, the accuracy of cloud optical depth determination and estimation of droplet effective radius that are most essential to modeling solar fluxes. Rossow and Schiffer (1999) concluded that despite the progress in understanding of global cloudiness, there is still much work to be done for reconciling satellite and ground-based retrievals of cloud properties.

Our study focuses on the modeling of radiative quantities and their comparison to observations made under overcast skies consisting of single-layer low-level non-precipitating clouds. Modeling solar radiative transfer in a cloudy atmosphere is a complex problem. Numerous input data are needed to define a closed problem: atmospheric profiles of humidity and liquid water, temperature and pressure, cloud boundaries and cloud microphysics, concentration and optical properties of aerosol. Also, surface spectral albedo is a basic model input parameter, fundamental in affecting the transfer of solar radiation. As a secondary part of this study, field measurements of surface albedo for basic typical surface types within the Atmospheric Radiation Measurement (ARM) Southern Great Plains (SGP) area were taken during early spring, coincident with the ARM Enhanced Shortwave Experiment (ARESE) 2000 Intensive Operational Period (IOP). It is shown that in the case of spatially inhomogeneous surface reflectance, such as the area surrounding the Central Facility (CF), point-wise measurements of surface albedo have a limited value for adequate representation of the boundary condition at the surface level.

## Data Selection and Modeling

Data collected at the CF site in northern Oklahoma from late 1997 until August 1998 were analyzed for the presence of isolated, low-level, non-precipitating layers of clouds. Broadband measurements of downward surface fluxes from the Baseline Surface Radiation Network (BSRN) radiometer, cloud radar snapshots, and Surface Meteorological Observing System (SMOS) measurements provided the means for determining suitable cloud cases. The presence of clouds was detected if direct broadband flux  $< 5 \text{ W m}^{-2}$ . Rain/snow gauge measurements, a component of data collected by the SMOS, indicated whether or not precipitation events had occurred. When available, satellite-observed radiance fields from the Visible and Infrared Scanner (VIRS) aboard the Tropical Rainfall Measuring Mission (TRMM) satellite at visible and infrared wavelengths were used to identify the phase (water/ice) of the cloud field in the vicinity of the CF. Hourly weather observations collected by on-site personnel provided additional information, such as the state of the ground conditions at the site. Several days containing at least one hour of overcast conditions were deemed appropriate for this study, occurring during winter and early spring.

The final screening for selecting cases depended on the availability of high-resolution solar spectral irradiance data from the Rotating Shadowband Spectroradiometer (RSS) (360 to 1100nm, 1024 channels). This instrument was developed at the Atmospheric Sciences Research Center at the State University of New York at Albany and has been operating at the CF site since August 1997 (Harrison et al. 1998). The latest version of the MODTRAN4 radiative transfer code (Anderson et al. 1999) was used. Radiosonde soundings provided atmospheric profiles of pressure, temperature, and water vapor. Total column amounts of water vapor and liquid water were available from microwave radiometer (MWR) retrievals. Water vapor mixing ratio profiles were calculated from the humidity, pressure and temperature profiles and scaled to MWR retrievals. Satellite data from Total Ozone Mapping Spectrometer (TOMS) provided ozone column amount. Initial values of surface albedo were obtained from the Multi-filter Rotating Shadowband Radiometer (MFRSR). Cloud top boundaries were determined using reflectivity observed by ground-based cloud profile radar. A threshold method was used whereby the background noise level was subtracted from the calibrated power signal. The cloud layer locations were determined at heights where the subtracted signal changed sign. Ceilometer observations were also used to validate the cloud base height. For those times of the year when insect contamination is greatest, determination of cloud top height from radar becomes difficult. In these cases, cloud top height was estimated from radiosonde soundings at the altitude where the relative humidity exceeds 94%.

Once cloud boundaries were found, vertical profiles of liquid water content were derived. Frisch et al. (1995) offered a relatively simple method for deriving the vertical liquid water content for stratus cloud, based on the knowledge of cloud boundaries, reflectivity  $Z$  ( $\text{m}^3$ ) from cloud radar, and integrated liquid water path (LWP) retrieved from a microwave radiometer. It is given by

$$q_1 = 0.3 \rho Z^{1/2} N^{1/2} \quad (1)$$

where  $N$  ( $m^{-3}$ ) is the number density of cloud droplets that is assumed to be constant with height,  $q_l$  is the liquid water content at level  $l$  and  $\rho$  is the density of water in  $g/m^3$ . Integrating this expression over the vertical height of the cloud yields the liquid water path. Given that the liquid water path is known,  $N$  can be expressed as

$$N = \{LWP / [0.3 \rho \int Z^{1/2} dl]\}^2. \quad (2)$$

Substituting this into [Eq. (1)] gives

$$q_l = (\rho LWP Z^{1/2}) / \int Z^{1/2} dl. \quad (3)$$

Liquid water content profiles for low-level water clouds can be determined from this expression.

Cloud microphysical properties were obtained from tuning the extinction coefficient at 500 nm to 550 nm to achieve agreement between the simulated and spectral downward surface flux from RSS in this spectral band. Effective radius,  $r_{eff}$ , was then calculated using this extinction coefficient and the LWP, following the relation

$$r_{eff} = 1.5 LWP / \tau, \quad (4)$$

where  $\tau$  is cloud optical depth, i.e., the extinction coefficient multiplied by the cloud layer thickness. For the cases considered here, effective radii varied from 6  $\mu m$  to 11  $\mu m$ , consistent with typical values for stratiform clouds estimated for the same region by Dong et al. (2000). Microphysical properties of the water cloud were modeled using Mie theory. The cases are summarized in Table 1.

Date	Time (UTC)	Column Amount (cm)			Cloud Position (km)	$t$ (550nm)	$R_{eff}$ (mm)
		WV	LW	$O_3$			
Feb 08	20h55m08s	1.36	4.8e-03	0.332	1.5 - 1.8	6.6	10.83
Mar 30	20h15m37s	2.46	2.0e-02	0.303	0.5 - 1.0	49.9	5.95
Apr 03	18h39m19s	1.45	3.2e-02	0.376	1.0 - 1.5	53.5	9.12

## Comparison Between Observation and Modeling

With observed and inferred atmospheric and cloud parameters, we first simulated downwelling spectral solar irradiance using nominal spectral surface albedos derived from synchronous MFRSR measurements. Since the MFRSR has much less spectral bands than the RSS, albedos between MFRSR channels were linearly interpolated to RSS bands. In some cases, agreement between modeling results and observations were good across the entire RSS spectrum. For several cases in springtime, agreement for the visible part of the spectrum was reasonably good, while in the near-IR (NIR) region the difference was quite noticeable with an abrupt jump near the chlorophyll absorption band at 0.7  $\mu m$ . This separation between two spectral regions suggested that it has something to do with the representativeness of point-wise MFRSR-based albedo for simulations under cloudy conditions. Analysis of surface type distribution and surface reflectances from LANDSAT imagery revealed that this might

happen due to the inhomogeneity of surface albedo around the CF. The majority of the area surrounding the CF is covered by green wheat, whereas the area right below the tower equipped with the MFRSR and other instruments is old dry grass. Typical albedo spectra for these two types are shown in Figure 1. The measurements were taken in March 2000, coincident with the ARESE 2000 IOP. Field measurements were done for all typical surface types within the ARM SGP region. The spectrometer S2000/PC2000 designed by Ocean Optics Inc. was used.

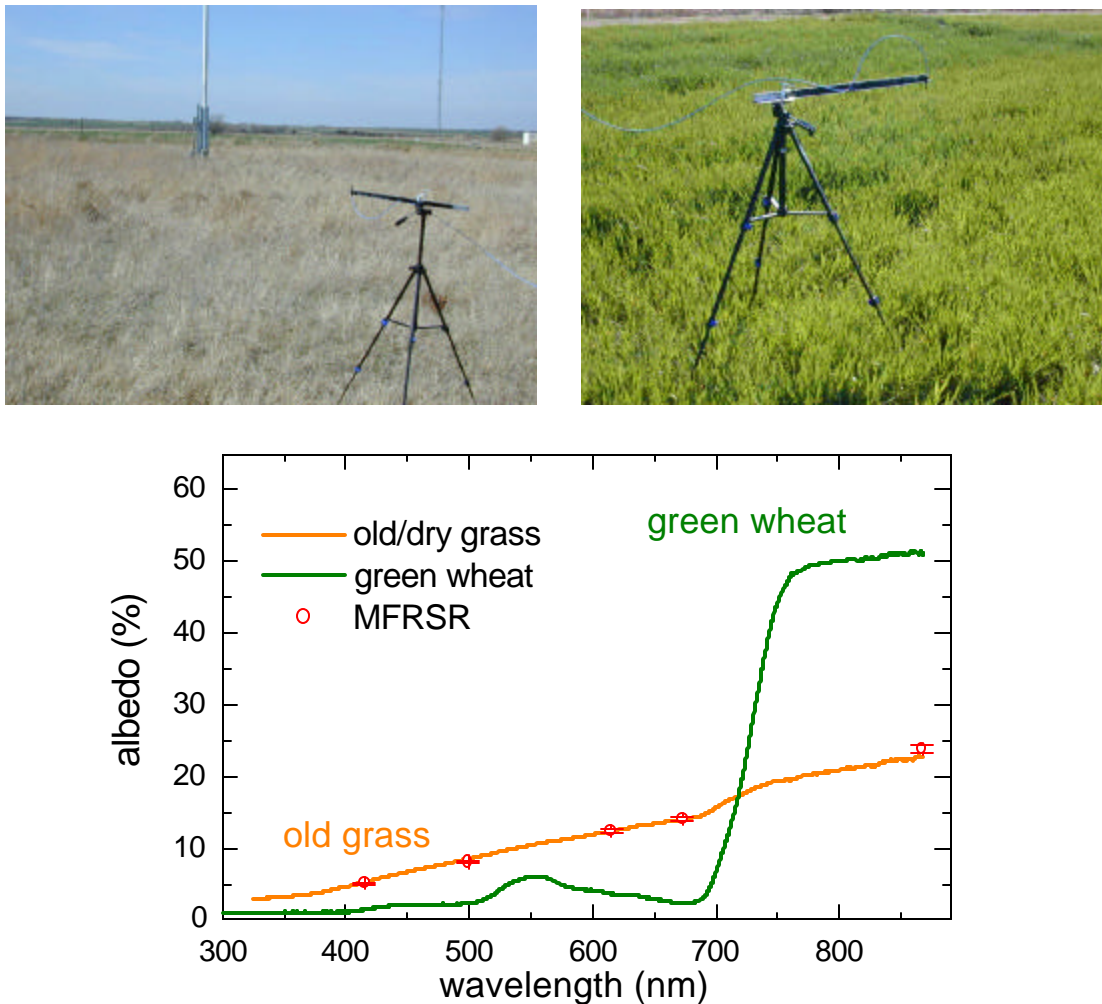


**Figure 1.** The top-left side of the figure shows a picture of a green wheat field, typical of the area around the CF. The top-right side of the figure shows old dry grass, the characteristic surface type in the vicinity of the MFRSR tower at the CF. The graph at the bottom shows corresponding measured spectra. The MFRSR data are in excellent agreement with our spectral measurements.

It is likely that the discrepancy in the NIR may be linked to the strong influence of green vegetation outside the viewing area of the MFRSR. To verify this hypothesis, an iterative procedure based on Newton's scheme was applied to determine the spectral surface albedos needed to make the model surface spectral fluxes agree with the RSS observed fluxes. It was found that in general, surface albedo

need to be increased substantially in the NIR range during the transition into the growing season. Figure 2 illustrates simulated spectral fluxes and the adjustments made to the surface albedo in order to achieve agreement with fluxes measured by the RSS.

Figure 3 compares areal-mean albedos to those measured by MFRSR and inferred from the comparison of downwelling spectral irradiance. Areal-mean albedo for different heights above the ground was then estimated using a hemispherical integration of the two-dimensional (2-D) albedo map. This 2-D albedo map was obtained as results of synthesis of our field spectral measurements and land cover classification made with LANDSAT imagery. The map looks quite inhomogeneous around the CF. Agreement between the areal-mean albedos and the inferred ones appears very good. This demonstrates that over an area characterized by spatially inhomogeneous surface albedo, such as that surrounding the CF, point-wise measurements of surface reflectance have limited value for adequate representation of the boundary condition at the surface level under overcast sky conditions. At the same time, point-wise measurements of spectral downwelling fluxes may be used to infer areal-mean spectral albedo.

Table 2 summarizes the comparisons of modeled and observed surface broadband downward flux and top-of-the-atmosphere (TOA) albedo. In general, the model using adjusted surface albedos reproduces broadband fluxes at the surface reasonably well and better than the model using MFRSR surface albedos, particularly in the early springtime. TOA albedos from both models compare fairly well with the CERES (Clouds and the Earth's Radiant Energy System) observations, except for the March 30 case; some high cloud may have been present after all and not accounted for in the modeling exercise.

From Table 3, in general, modeling data underestimate VIRS observations. Agreement at  $1.6 \mu\text{m}$  is better than for the red channel ( $0.63 \mu\text{m}$ ). The greatest differences with model calculations occur at  $3.75 \mu\text{m}$  where radiances are most sensitive to the effective radius of cloud droplets near the cloud top. In this study, a single value for effective radius was assumed for the whole cloud layer. The number of cases in comparison with satellite data is too small to make any decisive conclusions.

## Summary

Spectral and broadband fluxes at the surface and TOA radiances and albedos were calculated using measurements collected at the ARM SGP CF site as input into the MODTRAN radiative transfer code. The results were compared to RSS, BSRN downward surface fluxes, and VIRS and CERES satellite data, respectively. Low-level, single-layer, non-precipitating cloud cases were considered. Broadband total downward surface fluxes were reproduced well. In general, simulated TOA radiances underestimate VIRS observations. The greatest differences occurred at  $3.75 \mu\text{m}$  where radiances are most sensitive to the effective radius of cloud droplets near the cloud top. TOA albedos compared well with CERES data except for one case where there may have been some unnoticed high-level cloud, the presence of which was not included in the modeling.

The general location and strength of gaseous absorption lines in the spectrum of RSS surface measurements under cloudy conditions were adequately reproduced. Spectral fluxes at the surface showed significant sensitivity to the magnitude of the surface spectral albedo. Based on this, a method of reconciling modeled and observed spectral fluxes and retrieving surface spectral albedo from

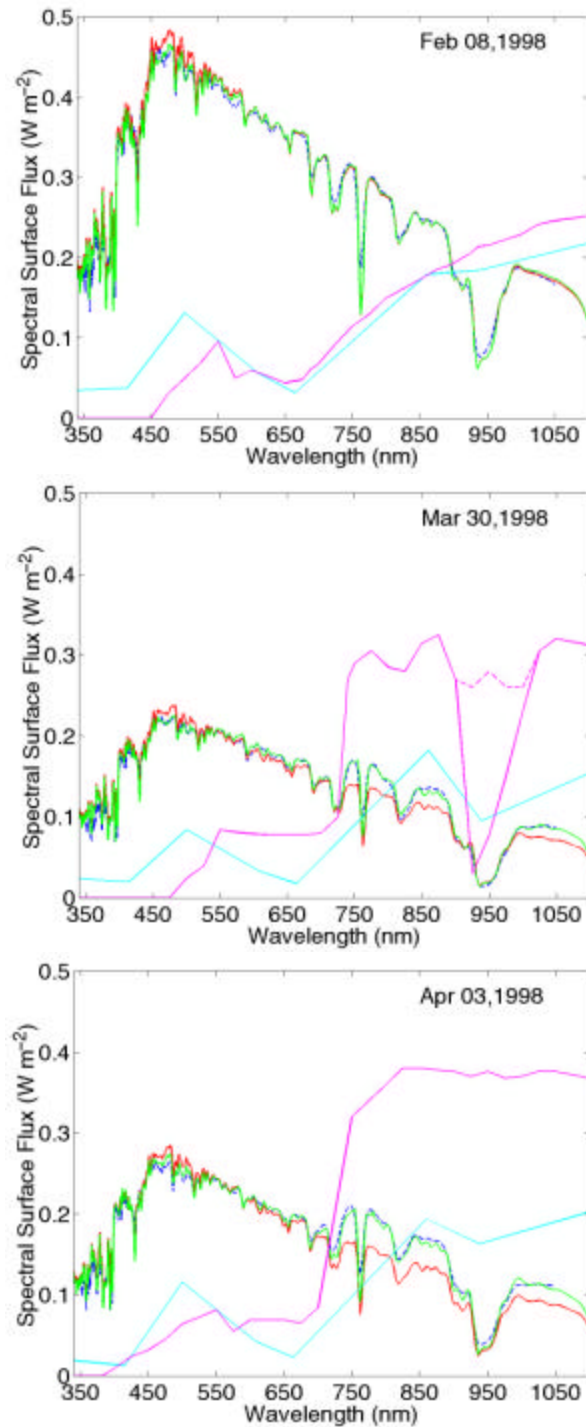


**Figure 2.** Surface flux as a function of wavelength for the three cases considered here. RSS measurements (blue dashed line), model simulations using MFRSR surface albedos (red line) and model simulations with adjusted surface albedos (green line) are shown. Also shown are the MFRSR surface albedos used (cyan line), as well as the adjusted surface albedos (magenta line).

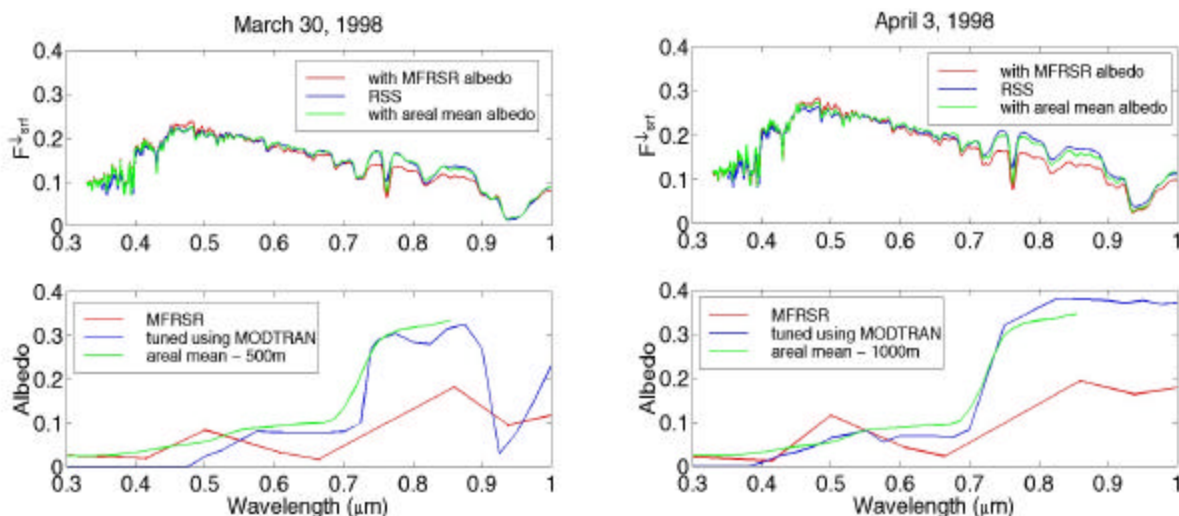


**Figure 3.** Model simulations using different surface albedos. For the areal means, altitude of sensor is at cloud base.

<b>Table 2.</b> Comparison of modeled and observed broadband downward surface flux and TOA albedo.						
Date	$F_{srf}^-$ ( $W m^{-2}$ )			TOA Albedo		
	BSRN	Model <sup>(a)</sup>	Model <sup>(b)</sup>	CERES	Model <sup>(a)</sup>	Model <sup>(b)</sup>
Feb 08	263.87	115.87	146.60	0.4660	0.7495	0.6253
Mar 30	256.49	116.45	143.79	0.4473	0.6219	0.6338
Apr 03	257.67	111.92	134.49	0.4487	0.6212	0.6326
(a) With adjusted surface albedos						
(b) With MFRSR surface albedos						

<b>Table 3.</b> Comparison of modeled and observed TOA radiances.						
Date	TOA Radiances ( $W cm^{-2} mm^{-1} sr^{-1}$ )					
	0.63 mm		1.6 mm		3.75 mm	
	VIRS	Model	VIRS	Model	VIRS	Model
Feb 08	1.17e-02	1.34e-02	1.85e-03	1.90e-03	5.42e-05	3.90e-05
Mar 30	3.64e-02	2.81e-02	3.46e-03	3.16e-03	6.48e-05	4.86e-05
Apr 03	3.69e-02	2.99e-02	3.53e-03	2.81e-03	6.16e-05	3.58e-05

downward surface irradiance is offered. Retrieved albedo shows good agreement with an independent estimation based on field measurements. It is suggested that measurements of surface albedo made at the CF site may not always be representative for adequate modeling of solar radiative transfer in overcast sky conditions, especially during the transition into the growing season such as during the ARESE 2000 IOP.

## Acknowledgments

The research was supported under the U.S. Department of Energy's Atmospheric Radiation Measurement Program, Grant DE-FG02-97ER62361.

## Corresponding Author

Z. Li, [zhanqing.li@ccrs.nrcan.gc.ca](mailto:zhanqing.li@ccrs.nrcan.gc.ca), (613) 947 1311.

## References

- Anderson, G. P. et al., 1999: MODTRAN4: Radiative transfer modeling for remote sensing. *Proc. SPIE, Optics in Atmospheric Propagation and Adaptive Systems III*, 3866, pp. 2-10.
- Dong, X., et al., 2000: A 25-month database of stratus cloud properties generated from ground-based measurements at the Atmospheric Radiation Measurement Southern Great Plains Site. *J. Geophys. Res.*, **105**, 4529-4537.
- Frisch, A. S., C. W. Fairall, and J. B. Snider, 1995: Measurement of stratus cloud and drizzle parameters in ASTEX with a  $K_{\alpha}$ -band doppler radar and a microwave radiometer. *J. Atmos. Sci.*, **52**, 2788-2799.
- Harrison, L. C., J. J. Michalsky, Q. Min, and M. Beauharnois, 1998: Analysis of rotating shadowband spectroradiometer (RSS) data. In *Proceedings of the Eighth Atmospheric Radiation Measurement (ARM) Science Team Meeting*, DOE/ER-0738, pp. 321-328. U.S. Department of Energy, Washington, D.C. Available URL: [http://www.arm.gov/docs/documents/technical/conf\\_9803/harrison-98.pdf](http://www.arm.gov/docs/documents/technical/conf_9803/harrison-98.pdf)
- Li, Z., A. Trishchenko, H. W. Barker, G. L. Stephens, P. T. Partain, 1999: Analysis of Atmospheric Radiation Measurement (ARM) program's Enhanced Shortwave Experiment (ARESE) multiple data sets for studying cloud absorption. *J. Geophys. Res.*, **104**, 1,9127-1,9134.
- Rossow, W. B., and R. A. Schiffer, 1999: Advances in understanding clouds from ISCCP. *Bull. Amer. Meteor. Soc.*, **80**, 2261-2287.
- Stephens, G. L. and S. -C. Tsay, 1990: On the cloud absorption anomaly. *Q. J. R. Meteorol. Soc.*, **116**, 671-704.